Predicting population consequences of ocean climate change for an ecosystem sentinel, the seabird Cassin's auklet

SHAYE G. WOLF*, MARK A. SNYDER†, WILLIAM J. SYDEMAN‡, DANIEL F. DOAK§ and DONALD A. CROLL*

*Department of Ecology and Evolutionary Biology, University of California, Center for Ocean Health, 100 Shaffer Rd., Santa Cruz, CA 95060, USA, †Climate Change and Impacts Laboratory, Department of Earth and Planetary Sciences, University of California, 1156 High Street, Santa Cruz, CA 95064, USA, ‡Farallon Institute for Advanced Ecosystem Research, PO Box 750756, Petaluma, CA 94975, USA, §Department of Zoology and Physiology, University of Wyoming, 1000 E. University Ave., Laramie, WY 82072, USA

Abstract

Forecasting the ecological effects of climate change on marine species is critical for informing greenhouse gas mitigation targets and developing marine conservation strategies that remain effective and increase species' resilience under changing climate conditions. Highly productive coastal upwelling systems are predicted to experience substantial effects from climate change, making them priorities for ecological forecasting. We used a population modeling approach to examine the consequences of ocean climate change in the California Current upwelling ecosystem on the population growth rate of the planktivorous seabird Cassin's auklet (*Ptychoramphus aleuticus*), a demographically sensitive indicator of marine climate change. We use future climate projections for sea surface temperature and upwelling intensity from a regional climate model to forecast changes in the population growth rate of the auklet population at the important Farallon Island colony in central California. Our study projected that the auklet population growth rate will experience an absolute decline of 11–45% by the end of the century, placing this population on a trajectory toward extinction. In addition, future changes in upwelling intensity and timing of peak upwelling are likely to vary across auklet foraging regions in the California Current Ecosystem (CCE), producing a mosaic of climate conditions and ecological impacts across the auklet range. Overall, the Farallon Island Cassin's auklet population has been declining during recent decades, and ocean climate change in this century under a mid-level emissions scenario is projected to accelerate this decline, leading toward population extinction. Because our study species has proven to be a sensitive indicator of oceanographic conditions in the CCE and a powerful predictor of the abundance of other important predators (i.e. salmon), the significant impacts we predicted for the Cassin's auklet provide insights into the consequences that ocean climate change may have for other plankton predators in this system.

Keywords: California Current Ecosystem, Cassin's auklet, climate change, ocean, population dynamics, population model, seabird, stochastic

Received 23 June 2009; revised version received 29 October 2009 and accepted 7 January 2010

Introduction

Climate change is having significant effects on marine ecosystems, including changes in phenology, distribution, and demographic rates of species from plankton to top predators (Walther *et al.*, 2002; Hoegh-Guldberg, 2005; Harley *et al.*, 2006). Beyond documenting current changes, forecasting how future climate change will affect biodiversity has become a priority for informing mitigation strategies (i.e. setting greenhouse gas emissions targets) and adaptation strategies to maintain or increase the resilience of species to climate change (Hannah *et al.*, 2002; Botkin *et al.*, 2007). In marine systems, ecological forecasts can inform sustainable emissions targets, the planning and design of marine protected area networks, and adaptation strategies to facilitate species' movements and reduce climate and nonclimate (e.g. fisheries pressure, coastal development) stressors.

Currently ecological forecasting has largely focused on bio-climatic envelope modeling to predict changes in species' distributions under future climate scenarios (Araújo & Rahbek, 2006). Owing to the difficulties in measuring climatic influences on multiple population parameters (Ådahl *et al.*, 2006), few studies have attempted to forecast population responses to climate

Correspondence: Present address: S. G. Wolf, Center for Biological Diversity, 351 California Street, Suite 600, San Francisco, CA 94104, USA, tel. + 1 415 632 5301, fax + 1 415 436 9683, e-mail: swolf@biologicaldiversity.org

change (Hunter *et al.*, 2007; Jenouvrier *et al.*, 2009). However, climate conditions (Helmuth *et al.*, 2006) as well as population responses to climate conditions can vary across species' ranges (Saether *et al.*, 2003; Grosbois *et al.*, 2006; Cheal *et al.*, 2007; Wolf *et al.*, 2009), highlighting the importance of forecasting climate change impacts at the population level.

We use a population dynamics modeling approach coupled with a regional climate model (RCM) to forecast population change for an ecosystem sentinel, the seabird Cassin's auklet *Ptychoramphus aleuticus* inhabiting the California Current Ecosystem (CCE), a coastal upwelling ecosystem along the west coast of North America. Coastal upwelling systems are among the most productive marine ecosystems that are predicted to experience substantial effects from climate change (Snyder *et al.*, 2003; Diffenbaugh *et al.*, 2004), making them priorities for ecological forecasting.

The CCE is sensitive to changes in ocean temperature and in the timing and intensity of winds that influence biological productivity in this system. Productivity is largely driven by seasonal equatorward winds that drive the upwelling of cold, nutrient-rich water into the euphotic zone and stimulate phytoplankton production (Huyer, 1983). Decreases in upwelling-favorable winds and the influx of warm surface water, which occur during El Niño events, and delays in the onset of upwelling can have dramatic ecosystem consequences, including failures in breeding and recruitment, higher mortality, and population declines across trophic levels (Barber & Chavez, 1983; Sydeman *et al.*, 2006; Barth *et al.*, 2007). Recent RCMs for the CCE project that the timing and magnitude of upwelling will change significantly within this century (Snyder *et al.*, 2003; Auad *et al.*, 2006). Snyder *et al.* (2003) projected that future changes in upwelling will be heterogeneous temporally and spatially throughout the CCE, with increases in some regions and seasons, decreases in other regions and seasons, and delayed onset of upwelling in some areas, notably in the northern CCE.

Cassin's auklets have proven to be sensitive ecological indicators of ocean climate change in the CCE (Sydeman *et al.*, 2006; Lee *et al.*, 2007; Wolf *et al.*, 2009) as well powerful indicators of population change for other marine predators (i.e. Chinook salmon) in this system (Roth *et al.*, 2007), making them useful for ecological forecasting. Key demographic rates for Cassin's auklets have been linked to ocean climate indices (Bertram *et al.*, 2001, 2005; Lee *et al.*, 2007; Wolf *et al.*, 2009). The mechanisms underlying the relationships between auklet demography and ocean climate conditions – i.e. the linkages between oceanographic indices, auklet zooplankton prey, and auklet demographic rates – have also been well-studied (Bertram *et al.*, 2001; Abraham & Sydeman, 2004, 2006;

Hipfner, 2008). Precipitous declines in the Cassin's auklet population at the Farallon Islands (75% or more since the early 1970s) and in the world's largest Cassin's auklet colony in British Columbia (Bertram *et al.*, 2000) have been attributed to changing oceanographic conditions, making it a species of conservation concern due to climate change (Lee *et al.*, 2007).

Here we use climate projections for the end of the century from a RCM for the CCE to forecast changes in the population growth rate of one of the largest Cassin's auklet populations in the United States, Southeast Farallon Island. We also evaluate predicted ocean climate change for two other important Cassin's auklet populations – Castle Rock in northern California and San Miguel Island in southern California – to assess the potential consequences of climate change across the auklet range in California. Finally, we highlight the challenges in making ecological forecasts even when using high resolution climate models and a well-understood study species.

Materials and methods

Study site

Southeast Farallon Island (hereafter 'Farallon Island'), California (37.7°N, 123.00°W), supports one of the largest populations of Cassin's auklets in the United States estimated at 105 000 breeding birds in 1971 (Manuwal & Thoresen, 1993; Lee *et al.*, 2007). Under a cooperative agreement with US Fish and Wildlife Service which manages the Farallon National Wildlife Refuge, PRBO Conservation Science (formerly Point Reyes Bird Observatory) monitors this population; field methods are described in Pyle (2001), Abraham & Sydeman (2004), and Lee *et al.* (2007). Based on at-sea observations of auklets (Ainley *et al.*, 1990b; Yen *et al.*, 2004), mean and maximum foraging distances estimated for other auklet populations from telemetry data (Adams *et al.*, 2004; Boyd *et al.*, 2008), and evidence that the Farallon population is resident (Ainley *et al.*, 1990a), we approximated the foraging range for this population as a rectangle extending 80 km north-and-south and 60 km east-and-west of the colony (Fig. 1). Foraging ranges for Cassin's auklet breeding populations at Castle Rock (41.76°N, 124.25°W) in northern California and at San Miguel Island (34.08°N, 120.25°W) in the Channel Islands in southern California (Fig. 1) were approximated as polygons extending approximately 80 km north-and-south and east-and-west of these colonies.

Overall approach

First, we determined relationships between auklet demographic rates and oceanographic conditions in the foraging range of the Farallon auklet population using a 26-year dataset (1980–2005) from which both auklet survival and breeding success information was available. Second, we characterized oceanographic conditions in the Farallon auklet foraging range, as well as in
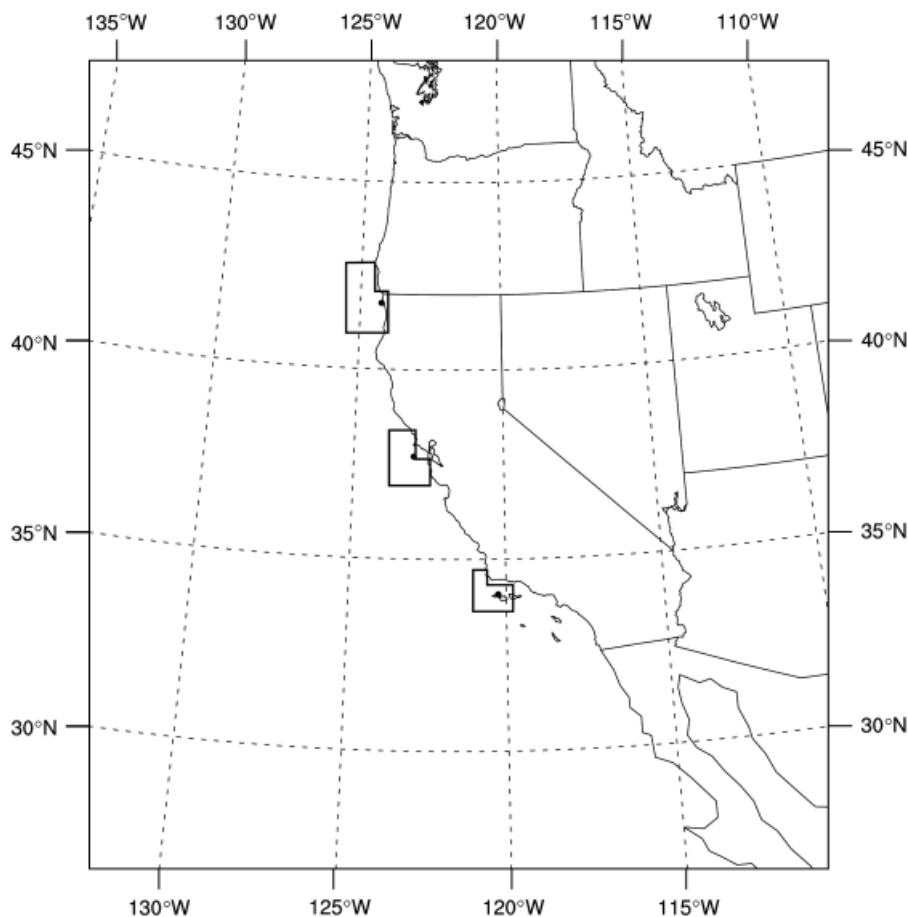
Fig. 1 Map of study regions. Auklet colony sites are denoted with a dot and the foraging region surrounding each colony is outlined as a polygon.

the two other study regions, from outputs of the RCM for the 'current' (1980–1999) and 'future' (2080–2099) model periods run under a mid-level emissions scenario. Third, we built a stochastic population dynamics model for the Farallon auklet population, with demographic rates modeled as a function of ocean climate conditions, to estimate the change in the auklet population growth rate between the current and future periods.

Relationships between auklet demographic rates and oceanographic conditions

Observed oceanographic conditions. We characterized oceanographic conditions in the auklet foraging range at Farallon Island using two indices: sea surface temperature (SST) and Bakun's upwelling index (UI) which approximates local upwelling intensity (Schwing *et al.*, 1996). We chose these indices because they are important indicators of productivity in this system, are significantly related to auklet demographic rates or auklet prey abundance (Abraham & Sydeman, 2004, 2006), and are available as outputs from the RCM. Oceanographic variables were averaged spatially over the auklet foraging range and temporally over the auklet breeding

season (March–August) and nonbreeding season (September of the prior year through February of the current year). We chose these time periods based on prior studies indicating that conditions during the winter are important for explaining annual variation in auklet survival (Lee *et al.*, 2007) and conditions during the breeding season are important for explaining annual variation in breeding success (Wolf *et al.*, 2009).

SST was derived from PATHFINDER version 5.0 data at 4 km spatial resolution provided by the NOAA Pacific Fisheries Environmental Laboratory (PFEL) (http://las.pfeg.noaa.gov/oceanWatch). Since Pathfinder data were available only from 1985 onward, we calculated monthly means for 1980–1984 from daily SST measurements taken from Farallon Island as described in Abraham & Sydeman (2004). Monthly Pathfinder and monthly Farallon Island means were highly correlated ($r^2 = 0.92$, 1985–1999, Pathfinder SST = $0.735 + 0.978 \times$ Farallon SST). We used this equation to estimate SST monthly means for 1980–1984 when Pathfinder data were unavailable to create a complete 1980–1999 SST time series. UIs were calculated from 6-hourly values of the Bakun's UI centered at 37.5°N, 123.5°W at 1° spatial resolution provided by the NOAA PFEL (http://las.pfeg.noaa.gov/las6_5/servlets/dataset).

Auklet demographic rates. We estimated annual auklet breeding success and survival rates during 1980–2005 using the long-term dataset from Farallon Island. Annual breeding success was calculated as the average number of chicks fledged per breeding pair from all breeding attempts, including relay attempts (eggs laid after the first breeding attempt fails) and second brood attempts (eggs laid after the first breeding attempt successfully fledges a chick).

We modeled and estimated apparent annual survival probability (φ) and recapture probability (ρ) in program MARK (White & Burnham, 1999) using live resighting data of marked individuals. Recapture probability was used as an estimate of breeding probability (i.e. the proportion of a population attempting to reproduce in a given year). All individuals were marked as chicks at 20–30 days of age. The first capture occasion was the year when a marked bird was first resighted and subsequent years were treated as recaptures. The resighting period was defined as the breeding period (March–August) each year during which individuals were assigned as present (observed in breeding attempts) or absent (not observed). Apparent survival probabilities include permanent emigration which we could not estimate from our data. We treated age as a constant in our models since all captured birds had attained reproductive maturity. In total, 349 individuals were resighted as breeders in nest boxes between 1982 and 2005.

We fitted a fully time-dependent Cormack–Jolly–Seber model with *year* as a categorical variable and *sex* as a group effect, with φ (*year* × *sex*) ρ (*year* × *sex*) as our global model. We tested the fit of the global model by estimating the variance inflation factor ($\hat{c}$), a measure of data overdispersion, calculated with two estimation methods: as the observed model deviance divided by the mean bootstrapped deviance, and as the mean observed $\hat{c}$ divided by the mean bootstrapped $\hat{c}$. For our global model, $\hat{c}$ was 1.17 and 1.34 for these two estimation methods, respectively, indicating little overdispersion. We also tested for goodness of fit (GOF) in U-CARE (Choquet *et al.*, 2005) which provided a low $\hat{c}$ estimate (1.09). The global test and component tests in U-CARE were not significant except for the directional test 2CT for trap dependence which was significant for males ($\chi^2_{19} = 42.19$, $P = 0.002$). Based on the GOF tests, we proceeded with our global model and used an inflation factor of 1.34 in the remaining analyses.

Relationships between oceanographic conditions and demographic rates. We used linear regression to test for significant relationships between mean annual breeding success and oceanographic conditions averaged over the breeding and nonbreeding seasons of 1980–2005. We used mark–recapture models to evaluate relationships between annual survival and recapture probabilities and oceanographic covariates. We created an *a priori* model set that included all reduced models of φ (*year* × *sex*) ρ (*year* × *sex*). We then tested the top models that included *year* by substituting *year* with the annual oceanographic indices, SST, UI, or SST and UI, for that year. Oceanographic indices were averaged over two different seasons (breeding and nonbreeding) using two different functional relationships: a linear function of the mean seasonal oceanographic index and

a nonlinear accelerating function of the mean seasonal oceanographic index (i.e. seasonal mean^2). We found the most parsimonious model for recapture probability while holding survival in its most parameterized form and then modeled survival with recapture probability in its most parsimonious form. The most parsimonious models were identified with Akaike's information criteria (AIC) corrected for small sample sizes (AIC$_c$) (Burnham & Anderson, 2002). In addition to the most parsimonious model (ΔAIC$_c$ = 0.0), models with ΔAIC$_c$ scores ≤ 2 can be considered to have received strong support. We used analysis of deviance (ANODEV) to determine the significance of covariate effects (Grosbois *et al.*, 2006) and calculated the amount of variation accounted for by covariates as [DEV (φ covariate)−DEV (φ constant)]/[DEV (φ time-dependent)−DEV (φ constant)], where DEV was the deviance for survival models with covariate, constant, and time effects, respectively (Skalski *et al.*, 1993).

RCM projections

We used the output of the RCM RegCM2.5 which has been well-validated for the California Current region (Snyder *et al.*, 2003) to project future ocean climate scenarios for the study sites. In order to provide realistic forcing, the RCM was driven by boundary conditions from a fully coupled global climate model, the National Center for Atmosphere Research Climate System Model, which includes outputs from component dynamic atmosphere, ocean, sea ice, and land surface models (Dai *et al.*, 2001). The model was run for two time periods, 1980–1999 and 2080–2099, with a horizontal resolution of 40×40 km, under a mid-level ACACIA-BAU (A Consortium for the Application of Climate Impact Assessments Business-as-Usual) emissions scenario. The RCM runs are discussed in greater detail in Snyder & Sloan (2005) and have previously been used to estimate the impact of climate change on endemic oaks in California (Kueppers *et al.*, 2005).

Output from the RCM was used to generate daily values for SST and the surface meridional and zonal wind components for each grid cell of each study site. To evaluate changes in upwelling, we calculated a daily UI, equivalent to the Bakun's UI (Bakun, 1973), from the meridional and zonal wind components. To do so, wind components were converted to wind stress τ by applying the following equation:

$$\tau = \rho_a \times C_d \times |v| \times v \ (\text{N m}^{-2}),$$

where ρ_a is air density, C_d is the empirical drag coefficient, and v is the wind vector with magnitude $|v|$ (Schwing *et al.*, 1996). Wind stress was used to estimate UI as described in Pickett & Schwing (2006):

$$\text{UI} = -mtv \times \tau/f \quad (\text{m}^3 \text{ s}^{-1} \text{ 100 m}^{-1} \text{ of coastline}),$$

where $-mtv$ is the mass to volume conversion (100 m coastline/1025 g m^{-3}) and f is the local Coriolus parameter. We calculated seasonal (breeding and nonbreeding) mean SST and UI for the current (1980–1999) and future (2080–2099) periods for each study region.

We used two methods to create sets of current and future oceanographic conditions for Farallon Island for use in the

auklet population model. In the first method, following Kueppers *et al.* (2005) and Stralberg *et al.* (2009), we used observed climate data during 1980–1999 for the current period. To create a climate projection for the future period, we averaged RCM monthly SST and UI outputs across years to produce one set of monthly mean values for the current and future periods. We calculated the differences between the RCM monthly means for the current and future periods and added these monthly mean anomalies to the observed monthly means of SST and UI for 1980–1999 to create the future climate projection (hereafter, 'method 1'). In the second method, we compared RCM monthly outputs with observed monthly means of SST and UI for the 1980–1999 period. We used linear regression between these datasets to develop a correction for the current RCM monthly outputs which we applied to generate corrected current climate conditions. We applied this same correction to the future RCM monthly outputs to create a corrected future climate projection (hereafter, 'method 2').

The RCM consistently overpredicted observed summer peaks in SST during 1980–1999. The method 2-corrected RCM outputs better fit the observed monthly SSTs but underestimated the variance in monthly SSTs (observed variance = 1.84; corrected RCM variance = 0.87, 1980–1999). Similarly, the RCM predicted higher peaks and troughs than reflected in the observed UIs for 1980–1999, and the method 2-corrected RCM outputs underestimated variance in observed monthly UIs (observed variance = 5142; corrected RCM variance = 667, 1980–1999). By using both methods for obtaining current and future climate scenarios, we attempted to bound likely climate effects on the Farallon auklet population: method 1 retained the observed variance in the current data and predicted similarly high variance in the future, whereas method 2 resulted in a more conservative projection of variance for both time periods (Appendix S1).

Auklet population model

We constructed a six-age class stochastic Leslie matrix to model Cassin's auklet population growth under current and future ocean climate conditions (Table 1, Fig. 2). The model follows a prebreeding census format in which each year of the model begins in March just before the breeding season and follows both male and female Cassin's auklets through the subsequent February. Males and females in the model have the same survival and breeding success rates. The six-age classes of the model are as follows: (1) 1-year-old nonbreeding sub-
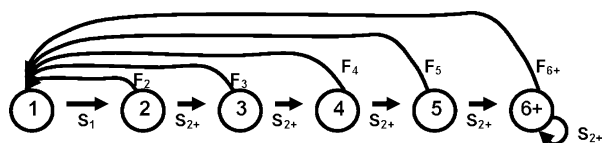
adults, (2) 2–5-year-old adults, a proportion of which are capable of breeding, and (3) 6-year-old and older adults, all of which are capable of breeding.

Survival of auklets age 2 and older (S_{2+}) was modeled as one of six alternative functions of SST and UI, as determined from the mark–recapture model. We were not able to estimate subadult survival probability for age class 1, and as a proxy, we used the subadult survival probability ($S_1 = 0.95 \times S_{2+}$) estimated for the Triangle Island, British Columbia, Cassin's auklet population (Bertram *et al.*, 2005). Juvenile survival ($Sjuv$, fledging to age class 1) was approximated as $Sjuv = 0.90 \times S_{2+}$ since survival in the first year of life is typically lower than in subsequent years (Nur & Sydeman, 1999).

Cassin's auklets in the model begin breeding as early as age 2 (Pyle, 2001), and we estimated the proportion of females in age classes 2 through 5 that are capable of breeding based on age of first breeding data for the Farallon population. The probability of breeding (i.e. probability that a female with breeding capability will attempt to breed in a given year) was approximated from the recapture probabilities for females generated by the mark–recapture model. For each year, a probability of breeding value was randomly drawn from a β distribution using the mean and variance estimated from the mark–recapture model and constrained by the correlation with that year's survival probability. Breeding success was modeled as a function of SST as determined by linear regression, and did not vary with age. The fecundity f of females in age class i for each year t was calculated as follows:

$$F_{i,t} = 0.5 \times \text{proportion breeding}_i$$
$$\times \text{probability of breeding}_t$$
$$\times \text{breeding success}_t \times Sjuv_t.$$

Auklet population growth rate under current and future ocean conditions

We ran the population model simulations for the current (1980–1999) and future (2080–2099) periods using the two sets of ocean climate projections generated using methods 1 and 2. In all models, breeding success was modeled as a function of SST, while adult survival was modeled as one of six alternative functions of ocean climate variables: SST (two models) or both SST and UI (four models) (Table 1). For the current and future values of SST and UI, all estimated survival and recapture rates fell within {0, 1}. Similarly, all estimated annual breeding success values fell within {0, 1} except for one of 19 values in the future period using climate projection method 1, and this exception, which was less than zero, was set to zero.

In each year of the model, a set of SST and UI values was randomly drawn from the set of 19 annual outputs for the current and future periods, respectively. We found no significant autocorrelation in the 19-year time series of SST and UI data using time lags of 1–5 years, indicating that stochastic model simulations that randomly selected annual sets of SST and UI values were appropriate. Each model was run for 50 years and 1000 simulations to generate a mean stochastic growth rate (λ) averaged across simulations. This approach

Fig. 2 Diagram of the age-based model developed for Cassin's auklets. Circles indicate age classes (1–6 +). Symbols associated with transition arrows indicate the types of transitions: S, the probability of surviving; F, fecundity, meaning the probability of producing a viable 1-year-old in the next generation.

Table 1 Cassin's auklet population matrix used for model simulations

---

$S_{i,t}$ for age classes $i = juv$, 1, and 2 + for each year t is defined as the following:

$$Sjuv_t = 0.90 \times S_{2+t}$$

$$S_{1t} = 0.95 \times S_{2+t}$$

$$S_{2+t} = \exp^{(5.517 - 0.025 \times (SSTnbd_t)^2)}/(1 + \exp^{(5.517 - 0.025 \times (SSTnbd_t)^2)})$$

$$= \exp^{(10.527 - 0.695 \times SSTnbd_t)}/(1 + \exp^{(10.527 - 0.695 \times SSTnbd_t)})$$

$$= \exp^{(6.415 - 0.0277 \times (SSTnbd_t)^2 - 0.0000499 \times (UInbd_t)^2)}/(1 + \exp^{(6.415 - 0.0277 \times (SSTnbd_t)^2 - 0.0000499 \times (UInbd_t)^2_t)})$$

$$= \exp^{(5.406 - 0.0244 \times (SSTnbd_t)^2 - 0.00208 \times UIbrd_t)}/(1 + \exp^{(5.406 - 0.0244 \times (SSTnbd_t)^2 - 0.00208 \times UIbrd_t)})$$

$$= \exp^{(6.287 - 0.0278 \times (SSTnbd_t)^2 - 0.00489 \times UInbd_t)}/(1 + \exp^{(6.287 - 0.0278 \times (SSTnbd_t)^2 - 0.00489 \times UInbd_t)})$$

$$= \exp^{(5.538 - 0.0244 \times (SSTnbd_t)^2 - 0.0000071 \times (UIbrd_t)^2)}/(1 + \exp^{(5.538 - 0.0244 \times (SSTnbd_t)^2 - 0.0000071 \times (UIbrd_t)^2_t)})$$

where $SSTnbd_t$ is the mean SST and $UInbd_t$ is the mean UI during the nonbreeding season, and $UIbrd_t$ is the mean UI during the breeding season in year t.

$F_{i,t} = f \times prop_i \times prob_t \times bs_t \times Sjuv_t$ for age classes $i = 1$–6 + where f is the proportion of the population that is female (assumed to be 0.5), $prop_i$ is the proportion of female breeding birds in age class i ($prop_2 = 0.25$, $prop_3 = 0.80$, $prop_4 = 0.92$, $prop_5 = 0.97$, $prop_{6+} = 1$), $prob_t$ is the probability of a female breeding in year t, bs_t is the breeding success (number of chicks fledged per female) in year t, and $Sjuv_t$ is the survival from fledging to 1-year-old in year t.

$$N_t \begin{bmatrix} 0 & F_2 & F_3 & F_4 & F_5 & F_{6+} \\ S_1 & 0 & 0 & 0 & 0 & 0 \\ 0 & S_{2+} & 0 & 0 & 0 & 0 \\ 0 & 0 & S_{2+} & 0 & 0 & 0 \\ 0 & 0 & 0 & S_{2+} & 0 & 0 \\ 0 & 0 & 0 & 0 & S_{2+} & S_{2+} \end{bmatrix}$$

N_t is population size in year t, S is age-specific survival, and F is age-specific fecundity; SST, sea surface temperature; UI, upwelling index.

illustrated the predicted range of population outcomes over a 50-year time horizon of conservation relevance. We also estimated asymptotic stochastic growth rates for each model scenario by running single long runs of 50 000 years. The absolute differences between these asymptotic rates and the means of the 50-year growth rates were all ≤ 0.004 and thus we report only the means and variances of the growth rates based on the 50-year simulations.

Results

Auklet demographic rates

Mean annual breeding success was significantly predicted by breeding season SST alone ($\beta = -0.21$, $P = 0.005$, $r^2 = 0.29$, adjusted $r^2 = 0.26$) (Fig. 3a), both breeding season SST and UI (SST $\beta = -0.16$; UI $\beta = 0.0015$; $P = 0.01$; $r^2 = 0.31$, adjusted $r^2 = 0.25$), and by breeding season UI alone ($\beta = 0.0034$, $P = 0.022$, $r^2 = 0.20$, adjusted $r^2 = 0.17$). Breeding success generally decreased with increasing SST, where the lowest chick production typically occurred during El Niño events with some exceptions (i.e. complete breeding failure occurred in 2005 independent of an El Niño event) (Fig. 3a). Relationships between breeding success and oceanographic conditions during the nonbreeding season

were not significant. Accordingly, adult breeding success in the stochastic population model was modeled as a function of breeding season SST alone because the adjusted r^2 values indicate that UI provided little explanatory power.

Annual variation in survival probability was most parsimoniously modeled as a function of oceanographic covariates, where survival probability did not differ between the sexes. Six survival models received considerable support (ΔAIC_c score ≤ 2), two with an SST covariate and four with SST and UI covariates (Appendix S2). ANODEV tests indicated that these covariates were significant (Appendix S2). In the best-supported survival model ($\Delta AIC_w = 0.212$), adult survival varied as a nonlinear function of nonbreeding season SST ($\beta = -0.0250$, 95% CI: -0.0347 to -0.0153), where the SST covariate accounted for 44% of annual variation in survival (Appendix S2). Survival probability decreased with increasing SST (Fig. 3b). Modeled survival probabilities were lowest during the anomalously warm 1983 and 1997 El Niño events when nonbreeding temperatures were 1.4–2 °C higher than the average during the 1980–2005 study period (Fig. 3b). In the best-supported model based on both SST and UI ($\Delta AIC_w = 0.103$), adult survival varied as a nonlinear

function of nonbreeding SST and nonbreeding UI (SST $\beta = -0.0277$, 95% CI: -0.0398 to -0.0156; UI $\beta = -0.0000499$, 95% CI: -0.00018 to 0.000078), where the UI covariate accounted for a small percentage (1.3%) of the annual variation in survival (Appendix S2). The most parsimonious models based on UI alone received very little support ($\Delta AIC_w = 0.00001$). Accordingly, adult survival probabilities in the stochastic population model were modeled as logit functions of SST alone (two models) and of both SST and UI (four models), as reported in Table 1. Adult recapture probability, a proxy of breeding probability, was most parsimoniously modeled as a function of *year* and *sex* instead of oceanographic conditions, where recapture probabilities for females were higher than for males.

RCM projections

At Farallon Island, mean annual SST increased by 1.97 °C between the current and future periods (Table 2) with the largest increases occurring during late summer and fall (Fig. 4a). Variance in mean annual SST increased only slightly in the future (+1.4%). Mean annual UI at Farallon Island decreased by 6% by the end of the century (Table 2), although changes in the UI varied considerably by month. UI increased in spring months (March–April) but declined during summer and fall months (May–October) (Fig. 4b). During the auklet breeding season from March to August, mean UI increased slightly (+0.9%) and UI variance increased considerably (27%). During the nonbreeding season from September to February, UI mean (−30%) and variance (−45%) decreased considerably. We detected no change in the mean date of upwelling onset since the transition to positive upwelling conditions occurred in April on average in both current and future projections.

Increases in SST were larger at the southern-most breeding site than at the northern-most site (Table 2).

Temporal changes in SST were rather synchronous across auklet breeding sites in California with the largest increases occurring in late summer to fall across sites (Table 2, Fig. 4a). However, changes in UI were heterogeneous across sites (Table 2, Fig. 4b). At Castle Rock, mean UI increased during both the breeding and nonbreeding seasons, whereas at San Miguel Island, mean UI increased during the breeding season and decreased during nonbreeding months. We detected no changes in the mean date of upwelling onset at Castle Rock or San Miguel.

Auklet population model

To assess the validity of our population model for the Farallon auklet population, we ran the model using observed values of SST and UI for 1980–1999. The deterministic population growth rates for the six best-supported models were extremely similar, ranging from 0.864 to 0.867, reflecting a ~13% annual decline in population size. Although annual estimates of population size are not available for this population, mean densities of occupied nests, which may provide a proxy of population size (Lee *et al.*, 2007), indicate a ~10% annual decline in population size between 1991 and 1999, which closely corresponds with the model predictions. Our estimates (mean ± SE) of annual adult survival probabilities during 1982–2005, which ranged from 0.763 ± 0.02, 0.763 ± 0.03, and 0.764 ± 0.03 for the six best-supported models, also compare well with estimates for Cassin's auklets at Farallon Island and elsewhere (Bertram *et al.*, 2005; Lee *et al.*, 2007).

Projected changes in the Farallon auklet population growth rate between current and future climate scenarios varied depending on the survival model and qclimate projections used (Table 3). When adult survival and breeding success were modeled as functions of SST using the best-supported survival model, the
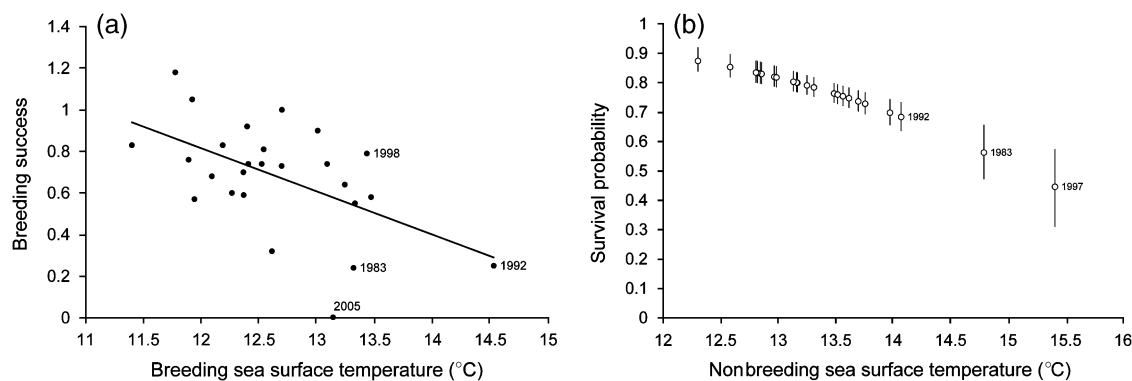

Fig. 3 Significant relationships between (a) annual mean breeding success (number of chicks fledged per pair) and sea surface temperature (SST) (°C) during the breeding season and (b) modeled annual adult survival probability and SST (°C) during the nonbreeding season. The El Niño events of 1992, 1983, and 1997–1998 are labeled.

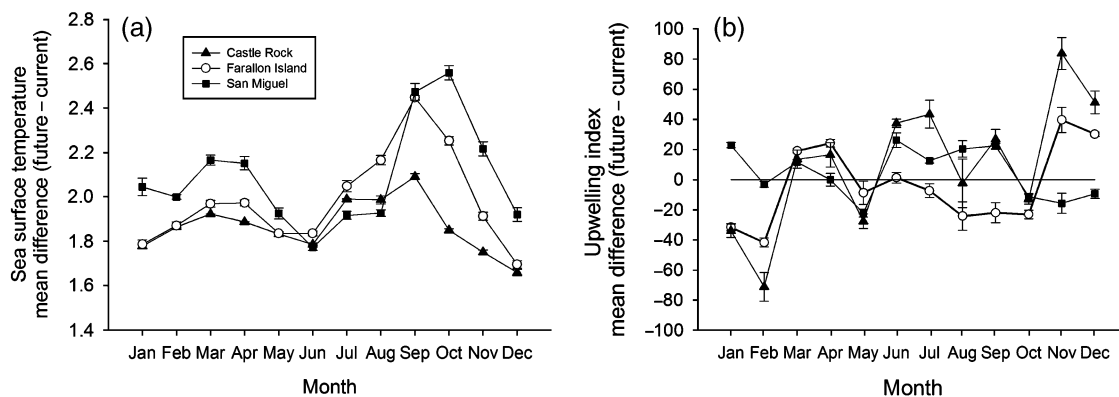**Fig. 4** Change in (a) monthly mean sea surface temperature (°C) and (b) monthly mean upwelling index ($m^3 s^{-1} 100 m^{-1}$ of coastline) between the future and current periods for the Castle Rock, Farallon Island, and San Miguel Island study regions. Error bars indicate SD.

Table 2 Annual and seasonal (breeding and nonbreeding season) changes in SST and UI between the future and current RCM projections averaged across each study region

	Castle Rock	Farallon	San Miguel
Annual changes			
SST	1.88 (+13.9%)	1.97 (+14.0%)	2.11 (+12.5%)
UI	10.33 (+24.5%)	−3.45 (−6.2%)	4.75 (+5.2%)
Seasonal changes			
SST breeding	1.90 (+13.4%)	1.97 (+12.8%)	1.98 (+11.0%)
SST nonbreeding	1.82 (+14.2%)	1.98 (+14.3%)	2.19 (+14.0%)
UI breeding	13.45 (+11.5%)	0.67 (+0.9%)	14.82 (+12.0%)
UI nonbreeding	8.75 (+24.3%)	−10.88 (−30.1%)	−10.27 (−17.2%)

Values in parentheses indicate percent changes between the current and future periods. Units are °C for SST and $m^3 s^{-1} 100 m^{-1}$ of coastline for UI.

SST, sea surface temperature; UI, upwelling index; RCM, regional climate model.

population growth rate decreased by 0.114 between the current and future periods under the more conservative climate projection (mean stochastic growth rate: $\lambda_{current} = 0.911 \pm 0.006$, $\lambda_{future} = 0.797 \pm 0.006$), and by 0.418 under the less conservative climate projection [mean stochastic growth rate: $\lambda_{current} = 0.863 \pm 0.021$, $\lambda_{future} = 0.445 \pm 0.023$ (Table 3; Fig. 5)]. Figure 5 illustrates the range of uncertainty in these projected population responses. Using the best-supported survival model based on SST and UI, the population growth rate decreased by 0.130 under the more conservative projection (mean stochastic growth rate: $\lambda_{current} = 0.853 \pm 0.006$, $\lambda_{future} = 0.723 \pm 0.005$) and by 0.445 under the less conservative projection (mean stochastic growth rate: $\lambda_{current} = 0.860 \pm 0.020$, $\lambda_{future} = 0.415 \pm 0.024$) (Table 3). There were similar decreases in the auklet population growth rate under the four remaining survival models that received considerable support (i.e. $\Delta AIC_c \leq 2$), with decreases of 0.11–0.13 under the more conservative climate projections and

0.40–0.45 under less conservative climate projections (Table 3).

Discussion

The Farallon Island Cassin's auklet population has already experienced a large-scale, climate-related population decline since the early 1970s (Lee *et al.*, 2007). Our model suggests that ocean climate change will accelerate this decline. Under a mid-level emissions scenario, the RCM projected significant ocean climate change in the Farallon Island auklet foraging range by the end of the century, including a large (∼2 °C) increase in SST year-round and an intensification of spring upwelling followed by an overall decrease in summer and winter upwelling. Based on these future ocean climate conditions, the auklet population growth rate at this important breeding site is projected to experience an absolute decline of 11–45% by the end of the century, which would lead to rapid population extirpation. Although

Table 3 Absolute change in mean stochastic population growth rate between 1980–1999 and 2080–2099 ($\lambda_{\text{future}} - \lambda_{\text{current}} = \Delta\lambda$) and current and future mean stochastic population growth rates shown in parentheses (current, future) for the Farallon auklet population using the six alternate survival models for which $\Delta\text{AIC}_c \leq 2$

Survival model	AIC$_c$ weight	Method 1 $\Delta\lambda$	Method 2 $\Delta\lambda$
φ ($SSTnbd^2$)	0.21	−0.418 (0.863, 0.445)	−0.114 (0.911, 0.797)
φ ($SSTnbd$)	0.16	−0.401 (0.863, 0.462)	−0.117 (0.910, 0.793)
φ ($SSTnbd^2$, $UInbd^2$)	0.10	−0.445 (0.860, 0.415)	−0.130 (0.853, 0.723)
φ ($SSTnbd^2$, $UIbrd$)	0.09	−0.409 (0.863, 0.454)	−0.115 (0.896, 0.781)
φ ($SSTnbd^2$, $UInbd$)	0.09	−0.447 (0.859, 0.412)	−0.130 (0.877, 0.747)
φ ($SSTnbd^2$, $UIbrd^2$)	0.09	−0.409 (0.863, 0.454)	−0.114 (0.902, 0.788)

Results are shown using the less conservative (method 1) and more conservative (method 2) climate projections. In all models, breeding success is modeled as a linear function of breeding season SST, recapture probability is modeled as a function of *year* and *sex*, and survival probability is modeled as a function of SST or SST and UI as denoted. *SSTnbd* denotes SST during the nonbreeding season, *UInbd* denotes UI during the nonbreeding season, and *UIbrd* denotes UI during the breeding season.

SST, sea surface temperature; UI, upwelling index; AIC$_c$, Akaike's information criteria corrected for small sample sizes.
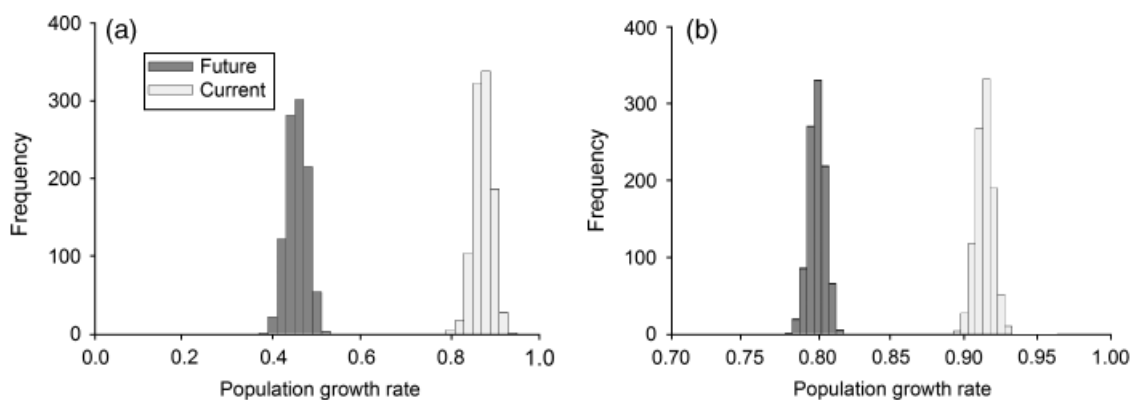

Fig. 5 Histogram of the stochastic population growth rate for the Farallon auklet population showing 1000 simulations run over 50 years during the current and future periods under the (a) less conservative (method 1) and (b) more conservative (method 2) climate projections, using the best supported model for breeding success and survival.

the exact values for average population change should not be taken too literally due to climate variability, now and projected into future, the overwhelming negative shifts in population growth with predicted climate change appear robust. Because breeding success of Farallon auklets covaries with population parameters of other important predators in the CCE (i.e. return rates of Sacramento River fall Chinook salmon) (Roth *et al.*, 2007), climate change-related impacts to auklet populations may be harbingers of effects on other plankton predators in this system.

Our RCM also indicates that future changes in upwelling intensity and timing of peak upwelling are likely to vary across California's most important auklet breeding sites. At San Miguel Island in southern California, mean increases in upwelling during the breeding season and mean decreases in upwelling during the nonbreeding season approximate patterns at Farallon

Island, suggesting that population consequences for auklets may be similar at these sites. At Castle Rock in northern California, increases in upwelling during the breeding and nonbreeding seasons could moderate the impacts of ocean warming, although increased wind-induced upwelling might also result in negative impacts on biological productivity as discussed further below. Overall, nonsynchronous changes in upwelling projected across the CCE are likely to produce a mosaic of climate impacts and auklet population responses across the system.

Improving population forecasts

Seabirds have proven to be important indicators of ocean climate dynamics in the CCE and elsewhere because they exhibit interannual variability in breeding parameters, survival, and abundance relative to

ocean climate variability (Briggs *et al.*, 1987; Ainley *et al.*, 1995; Sydeman *et al.*, 2001; Hyrenbach & Veit, 2003; Piatt *et al.*, 2007). Zooplanktivorous seabirds may be particularly informative indicators because they forage low in the tropic web and are more directly linked to primary production and the oceanographic processes that regulate this production. We projected ocean climate impacts on a zooplanktivorous seabird for which relationships between demography and climate variability are relatively well-understood. However, our population forecasts for this well-studied species were limited by the constraints of climate and population models. We discuss how the conservation utility of population projections could be enhanced by improvements to the RCM and population model.

Climate model limitations. A primary limitation of the RCM is its failure to capture some important physical indices that influence biological processes relevant to auklets in the CCE. The RCM simulates a subset of oceanographic processes important to biological productivity, principally SST and wind speed and direction. However, model measures of ocean temperature at depth (in addition to the surface) would provide a better index of how the upwelling of cold, nutrient-rich water would be affected by climate change. The warming of the upper ocean can inhibit the upward mixing of cold, nutrient-rich water by increasing thermal stratification, that is, by intensifying the density differences between the warmer surface layer and deeper, cold layer (Di Lorenzo & Miller, 2005; Harley *et al.*, 2006). In addition, surface warming can result in the deepening of the thermocline (i.e. a deepening of warmer waters), as is already being observed in coastal regions of the CCE (Palacios *et al.*, 2004; Di Lorenzo & Miller, 2005), meaning that upwelling-favorable winds are more likely to bring warm, nutrient-poor waters to the surface. Model projections of temperature at depth would allow a better understanding of whether the intensification of spring and summer upwelling-favorable winds projected for some regions would be sufficient to overcome increases in thermal stratification and a deepening of the thermocline to allow the upwelling of deep, nutrient-rich water.

Our approach was also limited by the use of one climate model and one realization of that model. The choice of climate models and emissions scenarios can influence forecasts of species responses to climate change, where the use of models that best-simulate observed climate conditions, multiple realizations of each model, and a range of emissions scenarios may provide a more robust approximation of species responses (Beaumont *et al.*, 2008). We chose the RCM because it was well-

validated for the CCE and provided good simulations of current climate variability at spatial scales relevant to auklets. However, our projections would be improved by using a wider range of models and emissions scenarios.

Population model limitations. Our population model could be improved by a better understanding of (1) additional factors that affect auklet demographic rates; (2) biological responses to novel combinations of physical conditions; (3) biological responses to changes in the timing of physical processes; and (4) auklet movement potential and changes in species interactions under changing climate conditions. Consistent with the large body of studies that have detected significant relationships between seabird demographic rates and ocean climate variables, our study found that seasonal SST explained 44% of the variation in annual adult survival and 29% of the variation in annual breeding success. Nonetheless, the unaccounted-for variation in auklet demographic rates indicates that our model did not capture all factors important to auklet demography. It is possible that ocean climate indices not used in this study may provide better explanatory power – for example, sea surface height (Wolf *et al.*, 2009) or basin scale indices (Lee *et al.*, 2007). For Farallon auklets, predation by western gulls (*Larus occidentalis*) may have some influence on survival and breeding success, but currently there is little evidence that many factors that have been shown to influence seabird demography (i.e. fisheries depletion of prey, fisheries bycatch of birds, disease, introduced species, competition) significantly affect Farallon auklets. It is also likely that even with the best information, a substantial fraction of the process variance in demographic rates will remain unexplainable for most populations. In this case, another way to improve predictions would be to incorporate both assignable and unassignable annual variance in demographic rates into model predictions (Bakker *et al.*, 2009).

In our model, the Farallon auklet population responded negatively to future increases in SST and decreases in upwelling within the foraging range because these conditions are similar to those that occur during strong modern-day El Niño events (i.e. 1982–1983, 1997–1998), when the slackening of upwelling-favorable winds coupled with the northward transport of warm water typically results in breeding failures and increased mortality of auklets. While some modeling studies suggest that the future Pacific Ocean may move into a prolonged El Niño-like state (Jackson, 2008; Lenton *et al.*, 2008), whether present-day El Niño events provide an appropriate proxy for future ocean conditions in the auklet foraging range is as yet uncertain. The RCM also projects novel ocean conditions in the foraging range of

northern California auklet populations – ocean warming accompanied by increases in upwelling-favorable winds – which are not analogous to modern-day conditions. How these nonanalogue conditions will affect biological processes is uncertain, although current biological responses to intense wind-driven upwelling in the CCE lend insights. First, although increased upwelling may help drive deeper nutrient-rich water to the surface, upwelling that is too vigorous or persistent may limit phytoplankton blooms (Kudela et al., 2008) and increase the advection of zooplankton larvae offshore, reducing their availability to coastal predators (Abraham & Sydeman, 2004; Harley et al., 2006). Accordingly, auklet euphausiid prey and many other marine organisms with planktonic life history stages appear to have an 'optimal environmental window' in which population growth initially increases with upwelling intensity but decreases when upwelling becomes too intense and persistent (Cury & Roy, 1989). In addition, increases in wind-driven upwelling have been linked to the emergence of anoxia and hypoxia in shelf waters of the northern CCE in recent years (Chan et al., 2008), which has resulted in the mortality of marine organisms (Grantham et al., 2004). Thus, although auklet survival and breeding success increase with intensified upwelling in our model, Cassin's auklets may not necessarily experience a benefit in regions projected to have more intense upwelling in the future.

Our population modeling effort would improve from a better understanding of how changes in the timing and length of the upwelling season will affect Cassin's auklet demographic rates. Auklet breeding success is sensitive to the timing of upwelling as evidenced by the unprecedented breeding failure of the Farallon population in 2005 following a 1-month delay in the onset of upwelling (Sydeman et al., 2006). Although our RCM projected no change in the onset of upwelling at Farallon Island, the model did project declines in the magnitude of summer and early fall upwelling which could result in a truncated upwelling season in the future. Upwelling near Farallon Island typically continues through October (Wolf et al., 2009) and may be important for sustaining production into winter. Importantly, in cold, productive years when coastal upwelling is prolonged late into the summer, Cassin's auklets are able to rear a second chick and substantially increase breeding success (Wolf et al., 2009). Thus, future declines in summer upwelling projected for Farallon Island could result in unfavorable conditions for second chick production, which is not well-captured by our model.

Finally, our population model does not integrate the capacity of auklets to respond to changing climate conditions by moving to more suitable locations or through adaptive change (phenotypic plasticity or microevolutionary change), nor does it incorporate altered responses of auklet prey, predators, and competitors to ocean climate change. In terms of movement, like many other seabirds Cassin's auklets exhibit high breeding-site fidelity, and predator-free breeding islands are scarce in many regions of the CCE, both of which may limit the auklet's ability to relocate to new breeding sites. Because the Farallon auklet population appears to forage in the vicinity of the colony year-round (Ainley et al., 1990a), Farallon auklets may also have a lower tendency to move to better foraging sites under changing climate conditions than assumed for many seabirds. Cassin's auklets exhibit variation in timing of breeding and selected prey species across widely spaced populations in the CCE (Wolf et al., 2009) which may indicate some potential to shift phenology and prey in relation to changing climate conditions. However, in years of delayed or disrupted upwelling, Farallon auklets tend to experience breeding failures even when they shift their timing of breeding (Sydeman et al., 2006), suggesting a more limited potential for successful responses to ocean climate change. Moreover, there is little evidence for evolutionary adaptation in vertebrates to climate warming (Gienapp et al., 2008). In terms of changing species interactions, one of the primary prey species for the Farallon auklet population, the krill *Euphausia pacifica*, is a cold water species whose availability and recruitment are linked to colder SSTs and stronger upwelling (Marinovic et al., 2002; Brinton & Townsend, 2003). Accordingly, the proportion of *E. pacifica* adults in the auklet diet increases in cold springs (Abraham & Sydeman, 2006). Therefore, future projected increases in ocean temperature and decreases in upwelling surrounding Farallon Island may result in reduced availability of key auklet prey species. Future modeling of climate change effects on auklet prey species will be important for strengthening insights into auklet population responses.

Conclusions

Our results suggest that projected ocean climate change under a mid-level emissions scenario is likely to result in the extirpation of the Farallon Island Cassin's auklet population since the oceanographic environment surrounding Farallon Island will not provide favorable year-round foraging conditions for auklets by the end of the century. In addition, predictable foraging locations for auklet populations across the CCE are likely to change, necessitating movement by auklet populations to find better breeding and wintering conditions. Overall, these results indicate that Cassin's auklet should be a priority for climate-integrated conservation strategies that increase the resilience of auklets to climate change by protecting colony sites across the auklet range and reducing nonclimate stressors at breeding colonies and at sea.

In a larger sense, despite the limitations of our models, these first order attempts to forecast the population consequences of climate change are useful in bounding the range of potential population change, setting emissions targets, and informing conservation strategies to help mitigate population declines for marine species.

References

Abraham CL, Sydeman WJ (2004) Ocean climate, euphausiids and auklet nesting: inter-annual trends and variation in phenology, diet, and growth of a planktivorous seabird, *Ptychoramphus aleuticus*. *Marine Ecology Progress Series*, **274**, 235–250.

Abraham CL, Sydeman WJ (2006) Prey-switching by Cassin's auklet *Ptychoramphus aleuticus* reveals seasonal climate-related cycles of *Euphausia pacifica* and *Thysanoessa spinifera*. *Marine Ecology Progress Series*, **313**, 271–283.

Ådahl E, Lundberg P, Jonzén N (2006) From climate change to population change: the need to consider annual life cycles. *Global Change Biology*, **12**, 1627–1633.

Adams J, Takekawa JY, Carter HR (2004) Foraging distance and home range of Cassin's auklets nesting at two colonies in the California Channel Islands. *Condor*, **106**, 618–637.

Ainley DG, Boekelheide RJ, Morrel SH, Strong CS (1990a) Cassin's auklet. In: *Seabirds of the Farallon Islands* (eds Ainley DG, Boekelheide RJ), pp. 306–338. Stanford University Press, Stanford, CA.

Ainley DG, Strong CS, Penniman TM, Boekelheide RJ (1990b) The feeding ecology of Farallon seabirds. In: *Seabirds of the Farallon Islands* (eds Ainley DG, Boekelheide RJ), pp. 51–127. Stanford University Press, Stanford, CA.

Ainley DG, Sydeman WJ, Norton J (1995) Upper trophic level predators indicate interannual negative and positive anomalies in the California Current food web. *Marine Ecology Progress Series*, **118**, 69–79.

Araújo MB, Rahbek C (2006) How does climate change affect biodiversity? *Science*, **313**, 1396–1397.

Auad G, Miller A, Di Lorenzo E (2006) Long-term forecast of oceanic conditions off California and their biological implications. *Journal of Geophysical Research-Oceans*, **111**, C09008, doi: 10.1029/2005JC003219.

Bakker VJ, Doak D, Roemer GW *et al.* (2009) Incorporating ecological drivers and uncertainty into a demographic population viability analysis for the island fox. *Ecological Monographs*, **79**, 77–108.

Bakun A (1973) *Coastal upwelling indices, West Coast of North America, 1946–71*. US Department of Commerce, NOAA Technical Report, NMFS SSRF-671, 103 pp.

Barber RT, Chavez FP (1983) Biological consequences of El Niño. *Science*, **222**, 1203–1210.

Barth JA, Menge BA, Lubchenco J *et al.* (2007) Delayed upwelling alters nearshore coastal ocean ecosystems in the northern California current. *Proceedings of the National Academy of Sciences of the United States of America*, **104**, 3719–3724.

Beaumont LJ, Hughes L, Pitman AJ (2008) Why is the choice of future climate scenarios for species distribution modelling important? *Ecology Letters*, **11**, 1135–1146.

Bertram DF, Harfenist A, Smith BD (2005) Ocean climate and El Niño impacts on survival of Cassin's auklets from upwelling and downwelling domains of British Columbia. *Canadian Journal of Fisheries and Aquatic Science*, **62**, 2841–2853.

Bertram DF, Jones IL, Cooch EG, Knechtel HA, Cooke F (2000) Survival rates of Cassin's and rhinoceros auklets at Triangle Island, British Columbia. *Condor*, **102**, 155–162.

Bertram DF, Mackas DL, McKinnell SM (2001) The seasonal cycle revisited: interannual variation and ecosystem consequences. *Progress in Oceanography*, **49**, 283–307.

Botkin DB, Saxe H, Araujo MB *et al.* (2007) Forecasting the effects of global warming on biodiversity. *Bioscience*, **57**, 227–236.

Boyd WS, McFarlane Tranquilla L, Ryder JL, Shisko SG, Bertram DF (2008) Variation in marine distributions of Cassin's auklets breeding at Triangle Island, British Columbia. *Auk*, **125**, 158–166.

Briggs KT, Tyler WB, Lewis DB, Carlson DR (1987) Bird communities at sea off California: 1975–1983. *Studies in Avian Biology*, **11**, 1–74.

Brinton E, Townsend A (2003) Decadal variability in abundances of the dominant euphausiid species in southern sectors of the California Current. *Deep-Sea Research Part II – Topical Studies in Oceanography*, **50**, 2449–2472.

Burnham KP, Anderson DR (2002) *Model Selection and Multimodel Inference*. Springer-Verlag, New York.

Chan F, Barth JA, Lubchenco J, Kirincich A, Weeks H, Peterson WT, Menge BA (2008) Emergence of anoxia in the California Current large marine ecosystem. *Science*, **319**, 920.

Cheal AJ, Delean S, Sweatman H, Thompson AA (2007) Spatial synchrony in coral reef fish populations and the influence of climate. *Ecology*, **88**, 158–169.

Choquet R, Reboulet AM, Lebreton JD, Giminez O, Pradel R (2005) *U-CARE 2.2 User's Manual*. CEFE, Montpelier.

Cury R, Roy C (1989) Optimal environmental window and pelagic fish recruitment success in upwelling areas. *Canadian Journal of Fisheries and Aquatic Science*, **46**, 670–680.

Dai A, Wigley TML, Boville A, Kiehl JT, Buja LE (2001) Climates of the twentieth and twenty-first centuries simulated by the NCAR climate system model. *Journal of Climate*, **14**, 485–519.

Diffenbaugh NS, Snyder MA, Sloan LC (2004) Could CO_2-induced land-cover feedbacks alter near-shore upwelling regimes? *Proceedings of the National Academy of Sciences of the United States of America*, **101**, 27–32.

Di Lorenzo E, Miller AJ (2005) The warming of the California Current System: dynamics and ecosystem implications. *Journal of Physical Oceanography*, **35**, 336–362.

Gienapp P, Teplitsky C, Alho JS, Mills A, Merila J (2008) Climate change and evolution: disentangling environmental and genetic responses. *Molecular Ecology*, **17**, 167–178.

Grantham BA, Chan F, Nielsen KJ *et al.* (2004) Upwelling-driven nearshore hypoxia signals ecosystem and oceanographic changes in the northeast Pacific. *Nature*, **429**, 749–754.

Grosbois V, Henry PY, Blondel J, Perret P, Lebreton JD, Thomas DW, Lambrechts MM (2006) Climate impacts on Mediterranean blue tit survival: an investigation across seasons and spatial scales. *Global Change Biology*, **12**, 2235–2249.

Hannah L, Midgley GF, Millar D (2002) Climate change-integrated conservation strategies. *Global Ecology and Biogeography*, **11**, 485–495.

Harley CDG, Hughes AR, Hultgren KM *et al.* (2006) The impacts of climate change in coastal marine systems. *Ecology Letters*, **9**, 228–241.

Helmuth B, Broitman BR, Blanchette CA *et al.* (2006) Mosaic patterns of thermal stress in the rocky intertidal zone: implications for climate change. *Ecological Monographs*, **76**, 461–479.

Hipfner JM (2008) Matches and mismatches: ocean climate, prey phenology, and breeding success in a zooplanktivorous seabird. *Marine Ecology Progress Series*, **368**, 295–304.

Hoegh-Guldberg O (2005) Climate change and marine ecosystems. In: *Climate Change and Biodiversity* (eds Lovejoy T, Hannah L), pp. 256–273. Yale University Press, New Haven.

Hunter CM, Caswell H, Runge MC, Regehr EV, Amstrup SC, Stirling I (2007) *Polar bears in the Southern Beaufort Sea II: Demography and Population Growth in Relation to Sea Ice Conditions. USGS Science Strategy to Support U.S. Fish and Wildlife Service Polar Bear Listing Decision*. US Geological Survey, Reston, VA.

Huyer A (1983) Coastal upwelling in the California Current System. *Progress in Oceanography*, **12**, 259–284.

Hyrenbach KD, Veit RR (2003) Ocean warming and seabird communities of the southern California Current System (1987–98): response at multiple temporal scales. *Deep-Sea Research II*, **50**, 2537–2565.

Jackson JBC (2008) Ecological extinction and evolution in the brave new ocean. *Proceedings of the National Academy of Sciences of the United States of America*, **105**, 11458–11465.

Jenouvrier S, Caswell H, Barbraud C, Holland M, Stroeve J, Weimerskirch H (2009) Demographic models and IPCC climate projections predict the decline of an emperor penguin population. *Proceedings of the National Academy of Sciences of the United States of America*, **106**, 1844–1847.

Kudela RM, Banas NS, Barth JA *et al.* (2008) New insights into controls and mechanisms of plankton productivity in coastal upwelling waters of the Northern California Current System. *Oceanography*, **21**, 46–59.

Kueppers LM, Snyder MA, Sloan LC, Zavaleta ES, Fulfrost B (2005) Modeled regional climate change and California endemic oak ranges. *Proceedings of the National Academy of Sciences of the United States of America*, **102**, 16281–16286.

Lee DE, Nur N, Sydeman WJ (2007) Climate and demography of the plantivorous Cassin's auklet *Ptychoramphus aleuticus* off northern California: implications for population change. *Journal of Animal Ecology*, **76**, 337–347.

Lenton TM, Held H, Kriegler E, Hall JW, Lucht W, Rahmstorf S, Schellnhuber HJ (2008) Tipping elements in the Earth's climate system. *Proceedings of the National Academy of Sciences of the United States of America*, **105**, 1786–1793.

Manuwal DA, Thoresen AC (1993) Cassin's auklet. *The Birds of North America*, **50**, 1–19.

Marinovic BB, Croll DA, Gong N, Bensen SR, Chavez FP (2002) Effects of the 1997–1999 El Niño and La Niña events on zooplankton abundance and euphausiid community composition within the Monterey Bay coastal upwelling system. *Progress in Oceanography*, **54**, 265–277.

Nur N, Sydeman WJ (1999) Demographic processes and population dynamic models of seabirds: implications for conservation and restoration. *Current Ornithology*, **15**, 149–188.

Palacios DM, Bograd SJ, Mendelssohn R, Schwing FB (2004) Long-term and seasonal trends in stratification in the California Current, 1950–1993. *Journal of Geophysical Research-Oceans*, **109**, C10016, doi:10.1029/2004JC002380.

Piatt J, Sydeman WJ, Wiese FK (2007) Introduction: a modern role for seabirds as indicators. *Marine Ecology Progress Series*, **352**, 199–204.

Pickett MH, Schwing FB (2006) Evaluating upwelling estimates off the west coast of North and South America. *Fisheries Oceanography*, **15**, 256–269.

Pyle P (2001) Age at first breeding and natal dispersal in a declining population of Cassin's auklet. *Auk*, **118**, 996–1007.

Roth JE, Mills KL, Sydeman WJ (2007) Chinook salmon (*Oncorhynchus tshawytscha*) – seabird covariation off central California and possible forecasting applications. *Canadian Journal of Fisheries and Aquatic Science*, **64**, 1080–1090.

Saether BE, Engen S, Moller AP *et al.* (2003) Climate variation and regional gradients in population dynamics of two hole-nesting passerines. *Proceedings of the Royal Society of London Series B-Biological Sciences*, **270**, 2397–2404.

Schwing FB, O'Farrell M, Steger J, Baltz K (1996) *Coastal Upwelling Indices, West Coast of North America 1946–1995*. NOAA Technical Memorandum NMFS-SWFSC-231, 32 pp.

Skalski JR, Hoffmann A, Smith SG (1993) Testing the significance of individual- and cohort-level covariates in animal survival studies. In: *Marked Individuals in the Study of Bird Populations* (eds Lebreton J-D, North PM), pp. 9–28. Birkhauser-Verlag, Basel, Switzerland.

Snyder M, Sloan LC, Diffenbaugh NS, Bell JL (2003) Future climate change and upwelling in the California Current. *Geophysical Research Letters*, **30**, 18–23.

Snyder MA, Sloan LC (2005) Transient future climate over the Western U.S. using a regional climate model. *Earth Interactions*, **9**, 1–21.

Stralberg D, Jongsomjit D, Howell CA, Snyder MA, Alexander JD, Wiens JA, Root TL (2009) Re-shuffling of species with climate disruptio: a no-analog future for California birds? *PLoS One*, **4**, e6825, doi:10.1371/journal.pone.0006825.

Sydeman WJ, Bradley RW, Warzybok P *et al.* (2006) Planktivorous auklet *Ptychoramphus aleuticus* responses to ocean climate, 2005: unusual atmospheric blocking? *Geophysical Research Letters*, **33**, L22S09, doi:10.1029/2006GL026736.

Sydeman WJ, Hester M, Thayer JE, Gress F, Martin P, Buffa J (2001) Climate change, reproductive performance and diet composition of marine birds in the southern California Current System, 1969–1997. *Progress in Oceanography*, **49**, 309–329.

Walther G, Post E, Convey P *et al.* (2002) Ecological responses to recent climate change. *Nature*, **416**, 389–395.

White GC, Burnham KP (1999) Program MARK: survival estimation from populations of marked animals. *Bird Study*, **46** (Suppl.), S120–S139.

Wolf SG, Sydeman WJ, Hipfner JM, Abraham CL, Tershy BR, Croll DA (2009) Range-wide reproductive consequences of ocean climate variability for the seabird Cassin's auklet. *Ecology*, **90**, 742–753.

Yen PPW, Sydeman WJ, Hyrenbach KD (2004) Marine bird and cetacean associations with bathymetric habitats and shallow-water topographies: implications for trophic transfer and conservation. *Journal of Marine Systems*, **50**, 79–99.

Supporting Information

Additional Supporting Information may be found in the online version of this article:

Appendix S1. Mean and variance of monthly SST and UI values for the current (1980–1999) and future (2080–2099) periods: (a) Current period; *observations* are observed monthly means for the current period created by method 1; *model corrected by observations* are corrected monthly RCM outputs for the current period created by method 2. (b) Future period; *observations plus anomalies* are observed monthly means added to RCM monthly mean anomalies created by method 1; *model corrected by observations* are corrected monthly RCM outputs for the future period created by method 2. *Model* denotes the raw RCM outputs for the current and future periods.

Appendix S2. Results of AICc model comparisons for survival models for which $\Delta AICc \leq 2$. *SST nbd* denotes SST during the non-breeding season, *UI nbd* denotes UI during the non-breeding season, and *UI brd* denotes UI during the breeding season. In all models, recapture probability is modeled as a function of *year* and *sex*: ρ (year, sex); k is the number of parameters. For each model, the *F* statistic and significance level for the ANODEV tests are reported, as well as the percentage of the variation accounted for by ocean climate covariate(s).

Please note: Wiley-Blackwell are not responsible for the content or functionality of any supporting materials supplied by the authors. Any queries (other than missing material) should be directed to the corresponding author for the article.